This is a postprint of: Fuel 84 (2005) 2048-2054

ALKALI ACTIVATION OF FLY ASHES. PART 1: EFFECT OF CURING CONDITIONS ON THE CARBONATION OF THE REACTION PRODUCTS

M. Criado, A. Palomo[1] and A. Fernández-Jiménez
Eduardo Torroja Institute (CSIC). 28080 Madrid. Spain

Abstract

This paper deals with the alkaline activation of fly ashes for the production of a novel cementitious material and with the effect of curing conditions on the nature of the reaction products. Curing procedures favouring carbonation process negatively affects the development of mechanical strength of this new alkaline cement. Carbonation of the system involves its pH modification and consequently the modification of the nature of the reaction products and the kinetics of reactions.

Keywords: *Fly ash, alkaline cement, curing, carbonation*

1. Introduction

The use of reinforced concrete in construction dates from the late nineteenth century. In the last one hundred plus years, as the construction industry has evolved in keeping with both overall technological development and market demands, Portland cement has become the most profusely used commodity on our planet.

Mass production of concrete and the concomitant mass manufacture of cement have, however, been observed to have a very negative environmental impact (almost one tonne of CO_2 is released into the atmosphere for every tonne of cement manufactured). Cement production is, moreover, a very energy-intensive process.

[1] *e-mail address: palomo@ietcc.csic.es

The foregoing problems have been addressed for a number of years from different perspectives, which very schematically, can be grouped in two major lines of action:

- Improvements in the efficiency of Portland cement manufacturing processes.
- Enhancement of certain features of Portland cement by including chemical additives, mineral admixtures, etc. to fresh concrete.

In short, it is clear that enormous efforts were made throughout the twentieth century to improve Portland cement concrete technology. At the same time, however, very limited research was conducted on new binders able to provide technical alternatives to conventional cement that could be produced at a fraction of the energy cost and environmental impact.

In this context, the idea of applying alkali activation to fly ash from steam plants, along the lines of previously successful applications of this process with other materials (1-8), was put forward in the Eduardo Torroja Institute (9).

Synoptically, the material proposed to replace Portland cement in concrete for use in construction is a binder prepared by mixing type F fly ash from coal-fired steam power plants with a highly alkaline solution. As this paste sets and hardens under moderate thermal conditions, the resulting precipitate is a gel with cementitious properties.

From the chemical standpoint alkali activation of fly ash is a process that differs widely from Portland cement hydration, but is very similar to the chemistry involved in the synthesis of a large groups of zeolites (10-11). The main reaction product in the alkali activation of fly ash is an alkaline aluminosilicate gel; that is to say a precursor of certain crystalline zeolite species (10). This product is structured around tetrahedrally co-ordinated silicon and aluminium, forming a polymer chain in which the Al^{3+} ions replace the Si^{4+} ions. The resulting net anionic charge is compensated by the capture of monovalent alkaline cations.

In technological terms, the long experience acquired with Portland cement concrete has revealed the importance of the conditions in which the product is manufactured and laid. The concrete curing process has a substantial impact on the quality and durability of the

material: it is during that process that the necessary environmental conditions must be created to keep the concrete moisture content at saturation or near saturation levels and thereby ensure full hydration of the cement (the ongoing hydration reactions in Portland cement are essential to increasing concrete mechanical strength and durability (12-15)).

In the alkali activation of fly ash, the objective pursued in the curing process is to attain conditions that optimise the polymerisation reactions (technologically speaking). The time required for appropriate alkali activation depends, in this case, on ash type and fineness, on the activating solution/fly ash ratio, on temperature, time, and on nature and concentration of the alkali activator (16,17).

2. Experimental

- *Materials*

The fly ash used in the present study was a Spanish ("CP") fly ash whose chemical composition is shown in Table 1. A very exhaustive characterisation of the fly ash was previously published by the authors (18). The initial chemical compositions of the activating solutions, in turn, are given in Table 2.

The reagents used to prepare the activators were laboratory grade: both the pellet-form NaOH (98% purity) and the sodium silicate, which had a density of 1.38 g/cc and a composition comprising 8.2% Na_2O, 27% SiO_2 and 64.8% H_2O, were supplied by Panreac S.A.

- *Method*

The fly ash was mixed with the different activating solutions (solutions A and B, see Table 2) at a constant "solution/ash" ratio of 0.4. After mixing, the pastes were immediately poured into prismatic moulds measuring 1x1x6 cm. These were then heated to 85ºC for different lengths of time: 5, 12, and 20 hours and 7 days.

The heating conditions were also varied to ascertain whether the curing atmosphere affected the mechanical and mineralogical evolution of the materials. Two alternative curing systems were studied:

> **method 1**: the moulds were placed in air-tight receptacles containing a certain amount of water, which was not, however, in contact with the moulds.
> **method 2**: the moulds were introduced directly into the oven alongside a porcelain capsule containing water.

After the materials were removed from the oven at the specified times, their mineralogical content was characterised by FTIR and XRD. The degree of reaction attained was also determined, using a method described in a preceding paper (19); ion chromatography was used to determine the soluble sodium content. The sodium was extracted from 3-g samples (previously vacuum-dried to a constant weight) that were placed in a flask with 250 cc of deionised water. The mixture was magnetically stirred for 3 h. Thereafter the system was filtered and water was added to the filtered solution to a total volume of 500 cc. This was the solution analysed for sodium content.

Finally, the mechanical properties of the different alkali-activated fly ash samples were determined by breaking the prismatic specimens with an Ibertest (Autotest – 200/10 – SW) compression tester.

3. Results

Figures 1 and 2 shows the diffractograms for all the materials prepared in the study (including the initial "CP" fly ash). All have a small halo in the 2θ =20-35º region, characteristic of amorphous and/or vitreous compounds. In all cases (except in the original ash) the presence of this halo is due, at least in part, to the alkali aluminosilicate gel formed as the primary reaction product in ash activation.

Generally speaking, the results of XRD analysis of the products indicated that quartz, mullite and magnetite were the chief crystalline phases (which were also found in the initial ash and apparently remained unaltered after activation). The other signals detected corresponded to zeolite structures such as hydroxysodalite ($Na_4Al_3Si_6O_{12}OH$)

and herschelite ($NaAlSi_2O_6.3H_2O$) or alkaline bicarbonates. The intensity of the bicarbonate signals increased with thermal curing time.

One important conclusion that may be drawn from the observation of the diffractograms in Figures 1 and 2 is that when sodium bicarbonate is formed then herschelite is not formed, and vice versa.

The infrared spectra for all the samples studied (including the spectrum for the original ash) are reproduced in Figures 3 and 4. The most relevant finding in these spectra is the shift observed in the T-O band (T=Si or Al). In the initial ash it appeared at $1078cm^{-1}$, moving from there to lower frequencies as a result of the formation of new reaction products associated with ongoing alkali activation. The shift recorded, to $998cm^{-1}$ (peak 4 in Figure 3) and 1013 cm^{-1} (peak 4 in Figure 4), is indicative of changes in the Si/Al ratio in the chief reaction product.

Tables 3, 4 and 5 list the band attributions for all the spectra shown in Figures 3 and 4.

Figures 5 and 6 show both the changes in the degree of reaction of these materials and their soluble sodium content over time. The curves for the materials cured using method 1 are given in Figure 5 and the ones for the materials cured using method 2 in Figure 6.

The curves in Figures 5 and 6 that refer specifically to degree of reaction over time (C1, D1, C2 and D2) indicate that the materials prepared through the method 1 reacted more fully than the ones prepared using curing method 2. The degree of reaction was likewise observed to increase over time, with a particularly steep rise in the first 20 hours. Thereafter and up to the end of the trial after 7 days, the degree of reaction rose very slowly.

Furthermore, the materials prepared using curing method 2 had a higher soluble sodium content which, generally speaking and as expected, declined with time.

Finally, Figure 7, which gives the mechanical strength curves for the materials studied, shows that whilst all compression strength values increased with reaction time (thermal

curing time), the ash activated and cured using method 1 had higher strength values than the ash activated and cured with method 2.

4. Discussion

4.1. General features of alkali activation of fly ash

The study of the alkali activation of fly ash as a method for synthesising new cementitious materials is gaining relevance in the scientific community. The characterisation of the alkaline aluminosilicate gels that comprise the chief reaction product of type F fly ash activation laid the grounds for a number of hypotheses regarding the mechanisms that govern such reactions, based essentially on currently accepted principles of zeolite chemistry (10). In this regard Nurayama et al. (20) established a general model for describing zeolite synthesis. According to these authors, the dissolution of Si^{4+} and Al^{3+} from coal fly ash is followed by the condensation of silicate and aluminate ions and the precipitation of the aluminosilicate gel, with zeolite crystallising after this second phase.

It is generally acknowledged (21-22) that there are two stages in zeolite synthesis mediated by the alkaline attack on aluminosilicate materials: A) a first nucleation stage in which the initial aluminosilicates are dissolved in the alkaline medium, favouring the formation of zeolite precursors and B) a second stage in which the various nuclei reach a critical size and begin to crystallise. When the ultimate purpose of fly ash activation is the synthesis of a cementitious material, however, the experimental conditions required include not only very high alkalinity but also a very low "alkaline dissolution/fly ash" ratio (9). In this case, therefore, the fly ash activation process may be regarded as being abruptly halted prior to zeolite crystallisation. In other words, a stable "zeolite precursor" forms at ambient conditions within a short reaction time; transformation to a well crystallised zeolite is only expected to take place in the very long term.

4.2. Impact of curing conditions and type of activator on ash activation mechanisms and the reaction products obtained

First of all, the various profiles observed in the diffractograms and IR spectra given in Figures 1, 2, 3 and 4 must be correctly interpreted. Specifically, X-ray diffraction patterns show that irrespective of the material studied (original or activated ash), it consists of a series of crystalline phases and one or several vitreous or amorphous phases. Moreover, the shift in the main band on the infrared spectrum for the original ash (located at 1078 cm^{-1}) to lower frequencies as the result of the alkaline attack (regardless of the duration of the thermal treatment or alkaline dissolution used) is an indication of the, at least partial, conversion of the vitreous component of the initial ash into the "zeolite precursor" mentioned above. Furthermore, this shift to a lower frequency, initially very abrupt (after only 5 hours of thermal curing), subsequently creeps upward (after 20 hours and 7 days of curing). This is interpreted as follows: in the very early stages, alkaline activation prompts the dissolution of a substantial fraction of the initial fly ash. As a result, an amorphous, metastable tecto-silicate with an Si/Al ratio of about 1 (23) is formed. After prolonged alkaline activation (24 hours, one week, etc.) the compound previously formed dissolves, to finally produce a "*zeolite precursor*" with a lower Al content (an Si/Al ratio of around 1.85 was deduced from the ^{29}Si NMR results (10)).

Another important finding that may be deduced from Figures 1, 2, 3 and 4 is related to the evolution of the zeolite crystalline phases formed (as by-products) during the reaction. Regardless of the curing procedure followed (method 1 or method 2), the alkaline solution used (A or B) or the duration of thermal treatment, the zeolite known as hydroxysodalite is always one of the crystalline phases present. It should nonetheless be noted that the materials obtained with curing method 1 and alkaline dissolution A had a substantially lower hydroxysodalite content than found for all the other cases (see Figure 1(a)). Another zeolite, namely herschelite, was primarily formed in this particular system.

The nature of the zeolites observed in these systems is, therefore, determined by the experimental conditions: concentration of the ionic species involved, pH of the medium, duration of thermal treatment, etc.

The identification of carbonate phases (essentially sodium bicarbonate) in a number of the samples studied, and especially in all the ones subjected to method 2, is particularly

relevant to the interpretation of the results. Irrespective of the duration of thermal treatment (5h, 12h, 20h or 7 days) and of the type of alkali activating solution used (A or B), all the spectra in Figure 4 show an intense band in the 1450 cm^{-1} region, characteristic of alkaline carbonates. The presence of such carbonates is likewise obvious in the XRD analyses.

Due to the highly basic nature of the systems studied, there is a strong thermodynamic tendency to reduce the pH (a phenomenon also present in Portland cement systems) by neutralisation with the surrounding medium, hence the carbonation reactions.

During the early stages of the process when the material is in contact with the atmosphere, carbonation occurs very rapidly, but as the material grows more compact it becomes more and more difficult for the CO_2 to penetrate the matrix; therefore the neutralisation rate declines substantially. The rate of carbonation has been shown to be highest with relative humidity ranging from 45% to 75% (24). Under such conditions, the CO_2 is dissolved in and spreads relatively readily through the material. With relative humidity values of over 80%, the pores become waterlogged and hinder the spread of the gas. If, on the contrary, the atmosphere is overly dry – relative humidity under 25% - the paucity of water available to dissolve the CO_2 prevents it from entering the system.

As a result of the formation of sodium bicarbonate, the system pH declines, rendering alkali activation less effective and therefore substantially reducing the rate of alkaline aluminosilicate gel formation.

The data on degree of reaction and soluble sodium given in Figures 5 and 6 confirm the foregoing. Hence, the specimens cured using method 1, in which the material is not in direct contact with the atmosphere, reach higher degrees of reaction than the specimens cured using method 2. Moreover, the reaction of part of the sodium present in the system in contact with the atmospheric CO_2 produces bicarbonates (very soluble species), thereby limiting, at least in part, the amount of this element that can be fixed to form alkaline aluminosilicate. This, in turn, slackens the pace of the activation reaction.

The effect of curing time on these materials is likewise very important. In the specific case of curing method 1, as the thermal treatment time increases, the quantity of

reaction product formed also increases (Figure 5); however, when method 2 is used, the results indicate that at the initial stages the amount of zeolite precursor formed remains nearly constant (see Figure 6) whilst at longer durations the percentage of soluble sodium decreases. The conclusion that may be drawn here is that the lowering of pH due to system carbonation reduces the ash activation rate but does not interrupt it altogether.

The mechanical strength curves concur with the rest of the results (Figure 7). The specimens cured with method 1 developed the greatest strength because alkaline activation progressed furthest in these specimens. In any event, compression strength values rose with reaction time regardless of the curing method used.

In short, all the results show that curing method 2 favours system carbonation, reducing the pH levels and therefore the ash activation rate.

Finally, reference must be made to the differences observed in the systems due to the use of different alkaline solutions - A or B – for fly ash activation. When the activating solution includes Na^{+} and soluble Si^{4+} alike, both elements are incorporated into the reaction products. The addition of waterglass to the activating solution favours polymerisation of the ionic species present in the system, a fact confirmed by the FTIR results: the reaction product obtained was Si-enriched. This would also explain the development of very high mechanical strength. It should nonetheless be noted that the NaOH + waterglass solution must be optimised not only as regards the SiO_2/Na_2O ratio but also with respect to system pH.

When the NaOH solution was used to activate the fly ash, the structure of the main reaction product was less polymerised, yet the mechanical strength values obtained for the specimens concerned were still satisfactory, perhaps as a result of the high OH^{-} content maintained in this system throughout the activation process.

5. Conclusion

The curing conditions play and important role in the manufacture of alkali activated fly ash cement. If the curing conditions are not suitable, a quick carbonation process can be

favoured. In this case, the initial carbonation of the system involves the reduction of the pH levels and therefore, the ash activation rate and the mechanical strength developments are notably slowed down. This initial carbonation process can be avoided by only controlling the environmental curing regime (high relative humidity).

Acknowledgements

To the Spanish Directorate General of Scientific Research for funding the project COO-1999-AX-038. To the Regional Government of Madrid for awarding a post-doctoral grant associated with this research. And finally to J.L. García and A. Gil for their co-operation in preparing the mechanical tests.

References

[1] B. Tailing and J. Brandster. "Present state and future of alkali-activated slag concretes". 3rd International Conference of Fly Ash, Silica Fume, Slag and Natural Pozzolans in Concrete. Tondheim (1989). SP 114-74, pp. 1519-1546.

[2] V.D. Glukhovsky, G.S. Rostovskaja and G.V. Rumyna. "High strength slag-alkaline cements". 7th International Congress on the Chemistry of Cement. Paris. (1980), 3, V-164-168,.

[3] I. Teoreanu "The interaction mechanism of blast furnace slag with water. The role of the activating agents". Il Cemento (1991), Nº2, pp 91-97.

[4] A. Fernandez-Jimenez and F Puertas. "Influencia de la concentración del activador sobre la cinética del proceso de activación de una escoria de alto horno", Mater Construction, (1997) 246, pp.31-41.

[5] A. Palomo and F.P. Glasser. "Chemically-bonded cementitious materials based on metakaolin" Br. Ceram. Trans. J. (1992) Vol 91, pp 107-112.

[6] Alonso S. and Palomo A. Alkaline activation of metakaolin and calcium hydroxide mixtures: influence of temperature, activator concentration and solids ratio. Materials Letters, (2001) vol 47, p.55-62

[7] J. Davidovits. "Geopolymers: Inorganic polymeric new materials" J. Thermal Anal. (1991) 37, pp.1633-1656.

[8] H. Xu and J.S.J. Van Deventer. "The geopolymerisation of aluminosilicate minerals". Int. J. Miner. Process (2000) 59, pp.247-266.

[9] Palomo A., Grutzeck M.W. and Blanco M.T. “Alkali activated fly ashes: A cement for the future”. Cement and Concrete Research, (1999) vol 29, p. 1323-1329.

[10] Palomo A., Alonso S., Fernández-Jiménez A., Sobrados I. and Sanz J. “Alkaline activation of fly ashes. A NMR study of the reaction products”. J. Am. Ceramic. Soc. (2004) 87, [6], pp.1141-1145.

[11] X. Querol, N. Moreno, J.C. Umaña, A. Alastuey, E. Hernandez, A. Lopez-Soler, F.Plana. “Synthesis of zeolites from coal fly ash: an overview”. International Journal of Coal Geology, (2002) vol 50, p. 413-423

[12] Bonavetti V., Donza H., Rahhal V. and Irassar E. “Influence of initial curing on the properties of concrete containing limestone blended cement”. Cement and Concrete Research, (2000) vol 30, p. 703-708

[13] Mannan M. A., Basri H. B., Zain M. F. M. and Islam M. N. “Effect of curing conditions on the properties of OPS-concrete”. Building and Environment, (2002), vol 37, p. 1167-1171

[14] Neville A. M. “Properties of Concrete”. Longman. 4th Edition (1995), p. 318-323

[15] Ho D.W. S., Cui Q. Y and Ritchie D. J. “Influence of humidity and curing time on the quality of concrete”. Cement and Concrete Research, (1989) vol 19, p. 457-464

[16] Fernández-Jiménez A. and Palomo A. “Alkali-activated fly ashes: properties and characteristics”. 11th International Congress on the Chemistry of Cement Durban, South Africa, (2003), vol.3, pp.1332-1340.

[17] M. Criado, A. Fernández-Jiménez. and A. Palomo “Microstructural features of fly ash based cementitious geopolymers”. Cement and Concrete Science. (2003) Edited by R. Mangabhai. University of Leeds.

[18] Fernández-Jiménez A. and Palomo A. “Characterisation of fly ashes. Potential reactivity as alkaline cements”. Fuel (2003), 82, pp. 2259-2265

[19] M.L. Granizo, S. Alonso, M.T. Blanco-Varela and A. Palomo “Alkaline activation of metakaolin. Effect of calcium hydroxide in the products of reaction" Jour. Am. Ceramic Society (2002) Vol.85, nº1 pp 225-231.

[20] N. Murayama, H. Yamamoto, J. Shibata, Mechanism of zeolite synthesis from coal fly ash by alkali hydrothermal reaction. Int. J. Miner. Process. (2002) 64, p.1-17,.

[21] R. Aiello, C. Collela, and R. Sersale, Molecular sieves; Advances in chemistry series 101; Am. Che. Soc. : Washington DC (1971), p 102

[22] E.M. Flanigen, Molecular sieves; Advances in chemistry series 121; Am. Che. Soc. : Washington DC (1973), p 119.

[23] A. Palomo, A. Fernández-Jimenez and M. Criado. “Geopolymers: one only chemical basis, some different microstructures”. *Mater Construcc.* (2004), Vol. 54, nº 275, pp.77-91.

[24] G. J. Verbeck “Carbonation of hydrated portland cement”. Am. Soc. Testing Material (1958). pp 17-36

Table 1.-Chemical analysis of "CP" fly ash (according to UNE 80-215-88 and UNE 80-225-93

	L.O.I	**I.R.**	**SiO_2**	**Al_2O_3**	**Fe_2O_3**	**CaO**	**MgO**	**SO_3**	**K_2O**	**Na_2O**	**TiO_2**	**Total**
%Wt	3.59	0.32	53.09	24.80	8.01	2.44	1.94	0.23	3.78	0.73	1.07	100

L.O.I. = Loss on ignition ; I.R = Insoluble residue in HCl (UNE

Table 2.-Chemical composition and pH of activating solutions.

	Na_2O (%)	**SiO_2 (%)**	**H_2O (%)**	**pH**
Solution A: NaOH	7.81	----------	92.19	13.93
Solution B: NaOH + waterglass	8.29	1.22	90.49	13.83

Table 3.- Bands on the FTIR spectrum of the original fly ash (before activation).

band	**cm^{-1}**	**Attribution**
4	1078	T-O bond (where T= Si or Al) stretching band
7	796 and 779	Quartz double band
9	693	Quartz band
10	668	O-Si-O bond band
12	555	Mullite band
14	460	SiO_4 tetrahedron ν_4 (O-Si-O) deformation band

Table 4.- Bands on the FTIR spectra of the activated fly ash.

band	cm^{-1}	Attribution
1	1450	Sodium bicarbonate band
2	1413	Sodium bicarbonate band
3	1080	Quartz band
4	1008 or 998	Alkaline aluminosilicate gel band (T-O, T= Si or Al)
5	881	Sodium bicarbonate deformation band
6	860	Sodium bicarbonate deformation band
7	796 and 779	Quartz double band
8	730	O-Si-O (zeolite species) bond band
9	696	Quartz band
10	668	O-Si-O (zeolite species) bond band
11	620	O-Si-O (zeolite species) bond band
12	560	Mullite band
13	512	O-Si-O (zeolite species) bond band
14	460	SiO_4 tetrahedron ν_4 (O-Si-O) deformation band

Table 5.- T-O bands shift for the A1, B1, A2 and B2 FTIR spectra.

A1	cm^{-1}	B1	cm^{-1}	A2	cm^{-1}	B2	cm^{-1}
5h	1008	**5h**	1012	**5h**	998	**5h**	998
12h	1008	**12h**	1012	**12h**	998	**12h**	998
20h	1008	**20h**	1012	**20h**	1007	**20h**	998
7d	1016	**7d**	1016	**7d**	1007	**7d**	1007

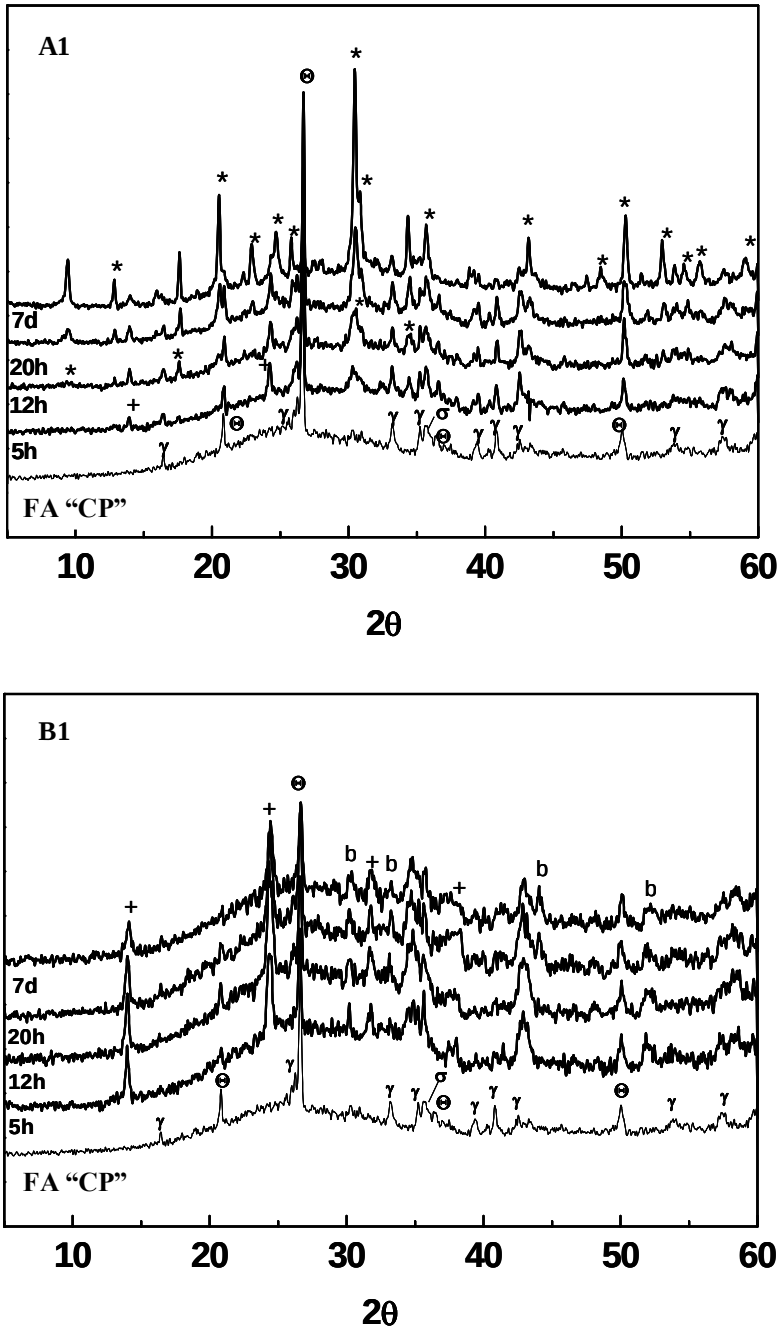

Θ: quartz, γ : mullite, σ : magnetite, + : hydroxysodalite,* : herschelite, b : sodium bicarbonate

Fig. 1 XRD spectra of alkali-activated fly ash cured in a oven at 85ºC using **method 1**, for: 5h, 12h, 20h and 7d. (**A1**) fly ash activated with solution A; (**B1**) fly ash activated with solution B.

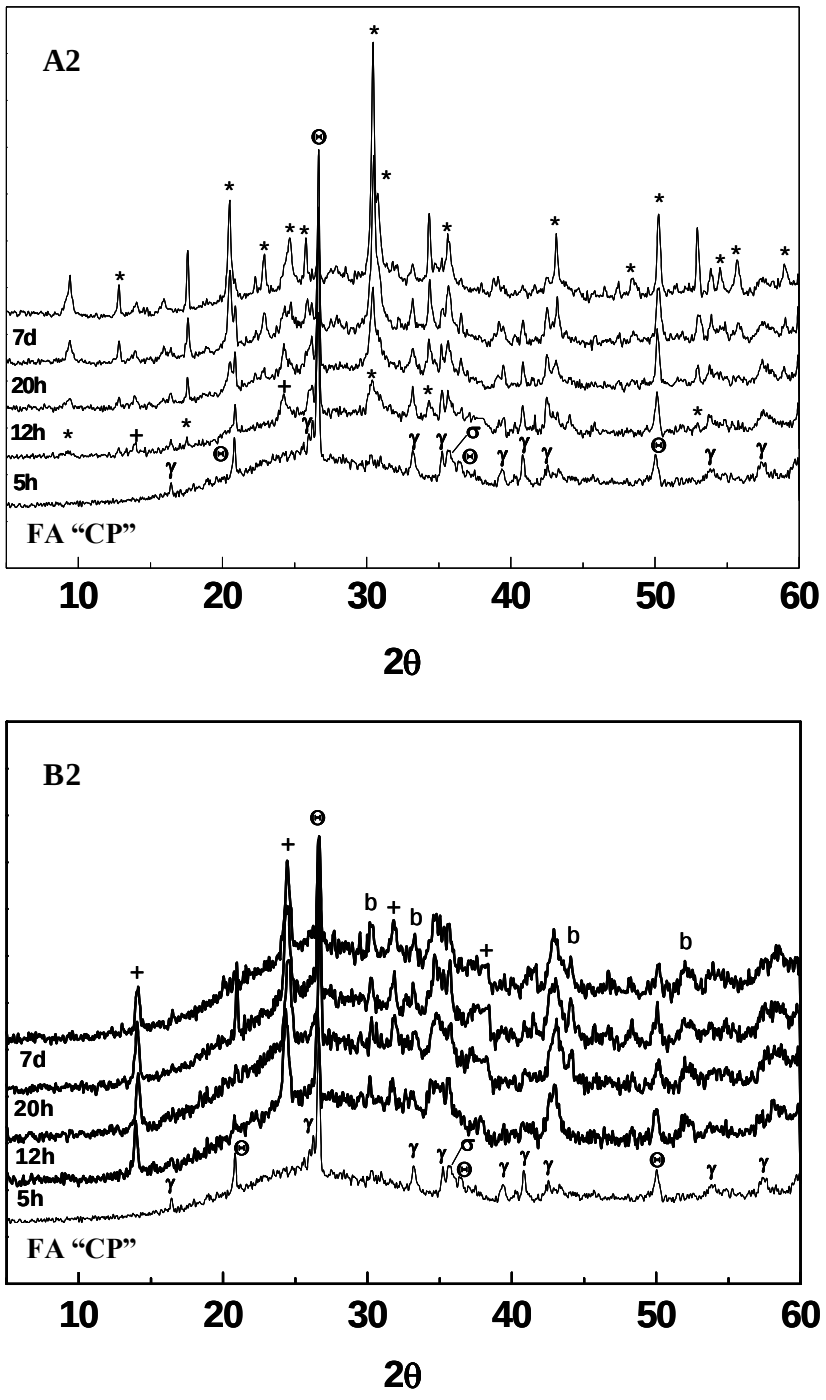

Θ: quartz, γ : mullite, σ : magnetite, + : hydroxysodalite,* : herschelite, b : sodium bicarbonate

Fig. 2 XRD spectra of alkali-activated fly ash cured in a oven at 85ºC using **method 2**, for: 5h, 12h, 20h and 7d. (**A2**) fly ash activated with solution A and cured. (**B2**) fly ash activated with solution B and cured using method 2.

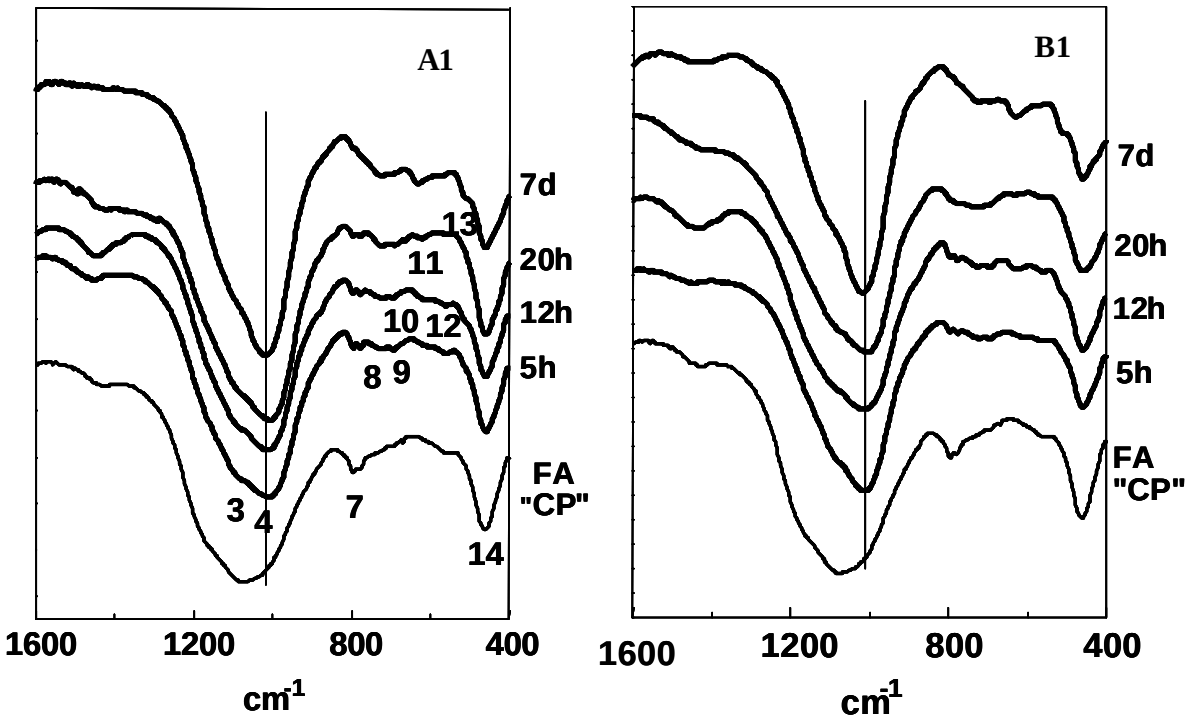

Fig. 3 FTIR spectra of alkali-activated fly ash cured in a oven at 85ºC using **method 1**, for: 5h, 12h, 20h and 7d. (**A1**) fly ash activated with solution A; (**B1**) fly ash activated with solution B.

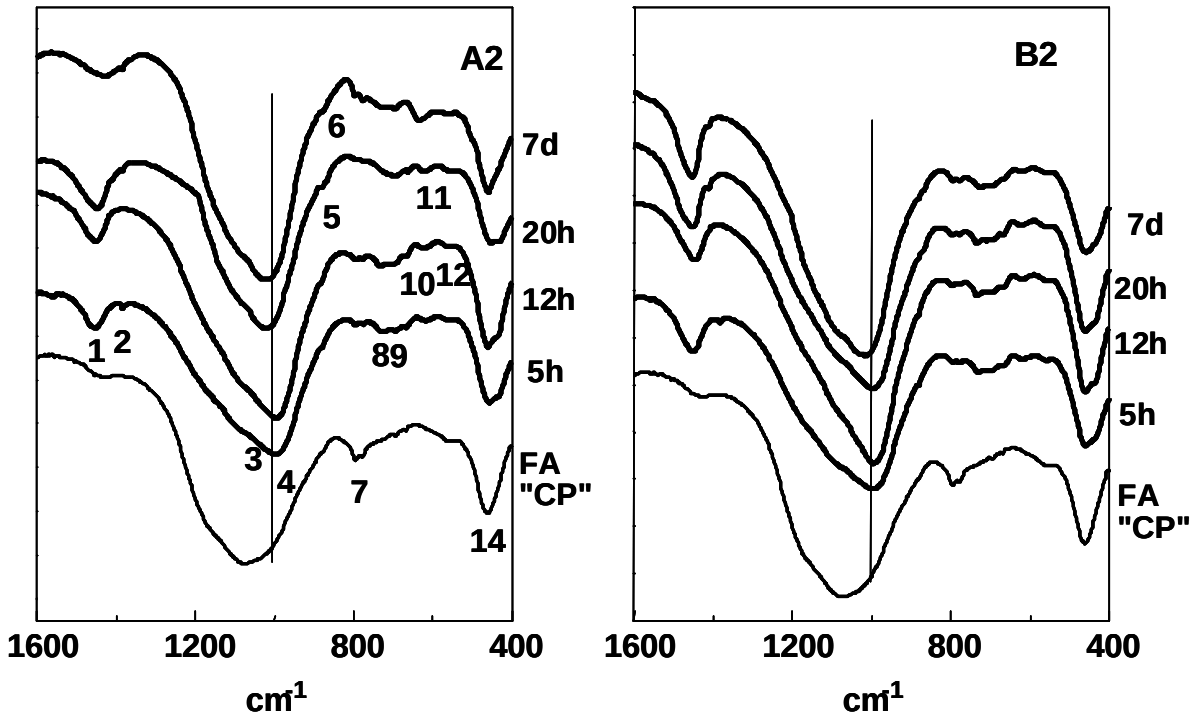

Fig.4 FTIR spectra of alkali-activated fly ash cured in a oven at 85ºC using **method 2**, for: 5h, 12h, 20h and 7d. (A2) fly ash activated with solution A; (B2) fly ash activated with solution B.

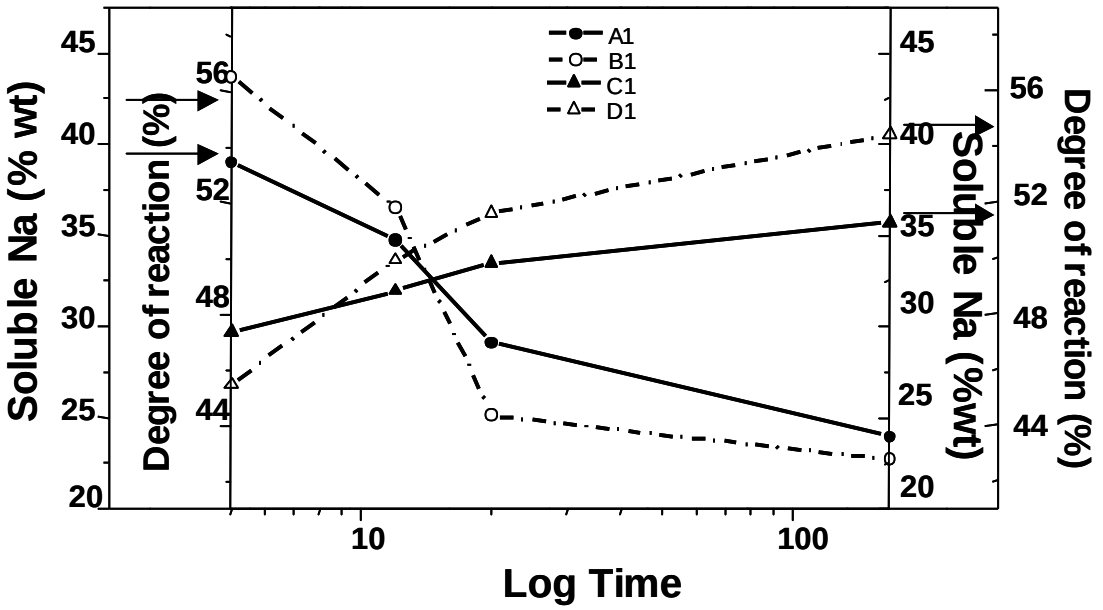

Fig. 5 Degree of reaction and soluble Na over time in materials treated using **method 1**; (**A1**) soluble Na in fly ash activated with solution A; (**B1**) soluble Na in fly ash activated with solution B; (**C1**) degree of reaction of fly ash activated with solution A; (**D1**) degree of reaction of fly ash activated with solution B.

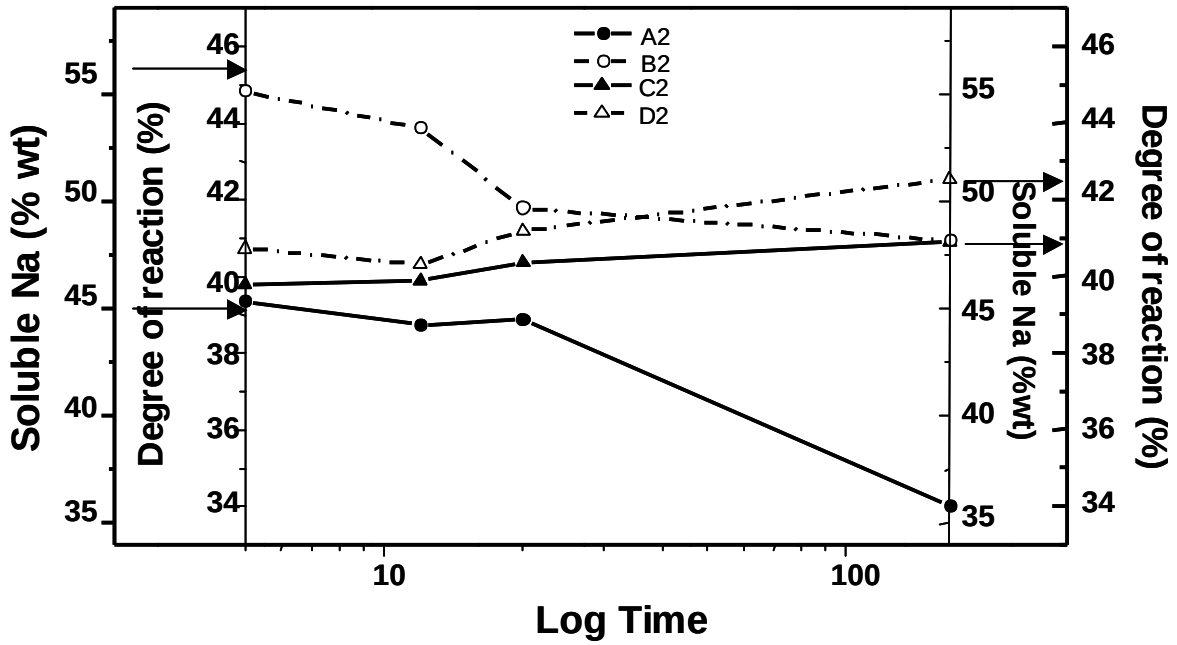

Fig. 6 Degree of reaction and soluble Na over time in materials treated using **method 2**; (**A2**) soluble Na in fly ash activated with solution A; (**B2**) soluble Na in fly ash activated with solution B; (**C2**) degree of reaction of fly ash activated with solution A; (**D2**) degree of reaction of fly ash activated with solution B.

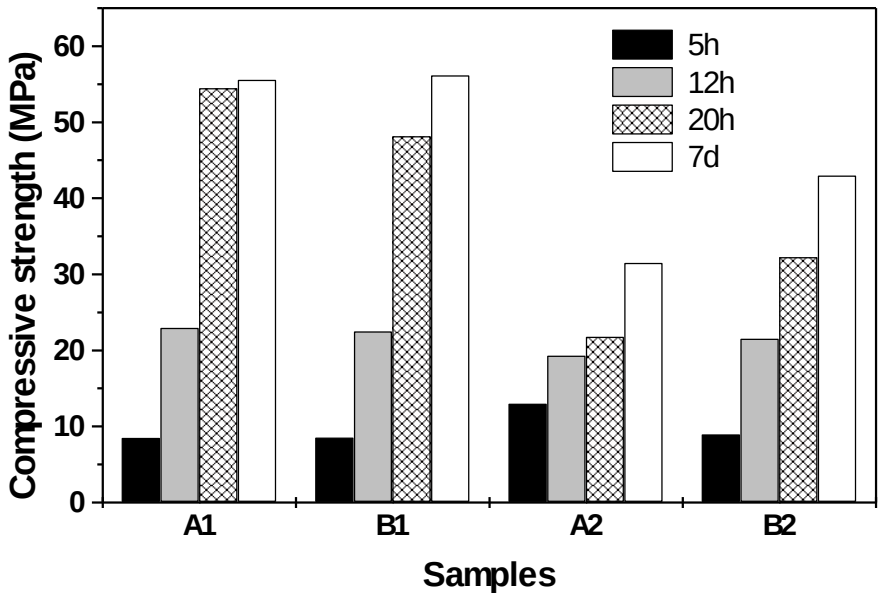

Fig. 7.- Compression strength values over time; (**A1**) fly ash activated with solution A and cured using method 1; (**B1**) fly ash activated with solution B and cured using method 1; (**A2**) fly ash activated with solution A and cured using method 2; (**B2**) fly ash activated with solution B and cured using method 2.